# Levels above the 19/2$^-$ isomer in $^{71}$Cu: Persistence of the $N = 40$ neutron shell gap

I. Stefanescu,[1,2,3] W. B. Walters,[1] R. V. F. Janssens,[2] N. Hoteling,[1,2] R. Broda,[4] M. P. Carpenter,[2] B. Fornal,[4] A. A. Hecht,[1,2] W. Krolas,[4,5] T. Lauritsen,[2] T. Pawlat,[4] D. Seweryniak,[2] J. R. Stone,[1,6] X. Wang,[2,7] A. Wöhr,[1,2] J. Wrzesinski,[4] and S. Zhu[2]

[1]*Department of Chemistry and Biochemistry, University of Maryland, College Park, Maryland 20742, USA*
[2]*Physics Division, Argonne National Laboratory, Argonne, Illinois 60439, USA*
[3]*Horia-Hulubei National Institute for Physics and Nuclear Engineering, P. O. Box MG-6, Bucharest, Romania*
[4]*Niewodniczanski Institute for Nuclear Physics, Krakow PL-31342, Poland*
[5]*Joint Institute for Heavy Ion Research, Oak Ridge, Tennessee 37831, USA*
[6]*Department of Physics, University of Oxford, OX1 3PU Oxford, United Kingdom*
[7]*Department of Physics, University of Notre Dame, Notre Dame, Indiana 46556, USA*

(Received 4 December 2008; published 26 March 2009)

Two prompt $\gamma$ rays of energies 2020 and 554 keV were observed in coincidence with delayed transitions depopulating the 19/2$^-$ isomer in the $Z = 29$, $N = 42$ $^{71}$Cu nucleus. The newly identified transitions are proposed to deexcite the 4776- and 5330-keV levels above the 19/2$^-$ isomer. Based on the comparison with the low-lying positive-parity states observed in the $Z = 42$, $N = 50$ $^{92}$Mo nucleus, spin and parity 23/2$^-$ are proposed for the 4776-keV level in $^{71}$Cu. The high-energy, 2020-keV transition is interpreted as arising from the breaking of the $N = 40$ neutron core. Shell-model calculations with a $^{56}$Ni core reproduce the (23/2$^-$) → (19/2$^-$) gap well, suggesting that the 23/2$^-$ state is dominated by $\pi p_{3/2}\nu((fp)^{10}(g_{9/2})^4)$ configurations. The present result constitutes further evidence supporting the view that the $N = 40$ subshell closure persists in $^{71}$Cu, herewith challenging recent suggestions that the coupling of two or more proton or neutron quasiparticles induces a large polarization of the $^{68}$Ni core.

DOI: 10.1103/PhysRevC.79.034319 PACS number(s): 23.20.Lv, 21.60.Cs, 27.50.+e, 23.35.+g

## I. INTRODUCTION

Since it was proposed in the eighties by Bernas *et al.* [1,2], the magic character of $^{68}$Ni has attracted much experimental and theoretical interest. In that work, the existence of the $N = 40$ subshell closure was suggested through the observation of an excited state at ∼2.2 MeV, proposed to correspond to the $2_1^+$ level, as well as through the presence of a low-lying $0_2^+$ state at 1770 keV. The two levels, populated in a two-proton pick-up reaction on a $^{70}$Zn target [1,2], were later firmly established by the results of a deep-inelastic measurement that fixed the energy of the $2_1^+$ state at 2.033 MeV [3].

The recent development of radioactive ion-beam facilities combined with advanced detection systems has provided a number of opportunities for further investigations of the properties of $^{68}$Ni as well as of the impact of the $N = 40$ subshell closure on the single-particle and collective properties of the neighboring nuclei. Beta-decay [4,5] and Coulomb excitation experiments with radioactive beams [6–8] have provided important evidence supporting the doubly magic character of $^{68}$Ni. However, the stabilizing effects of the $Z = 28$ shell and $N = 40$ subshell gaps were found to be very much localized around $^{68}$Ni as the unexpectedly large $B(E2)$ values observed at low-excitation energies in $^{70}$Ni [9] and $^{72}$Cu [7,10] as well as the low excitation energy of the $2^+$ state in $^{66}$Fe [11] and the newly observed 1/2$^-$ isomer in $^{67}$Co [12] were interpreted as clear indications for the weakening of the $N = 40$ subshell and/or $Z = 28$ shell closures when more than two-like quasiparticles are added to the $^{68}$Ni core. The quenching of the (sub)shell gap(s) was ascribed to the strong interaction between the $pf$ protons and $g_{9/2}$ neutrons that induces energy shifts of the single-particle orbitals thereby leading to an increased collectivity in neutron-rich nuclei beyond and below $^{68}$Ni [13].

This article reports on the identification of two excited levels on top of the 19/2$^-$ ($T_{1/2} \sim 0.26$ $\mu$s) isomer in $^{71}$Cu. This isomer was identified in deep-inelastic experiments performed at GANIL [14] and at the JAERI tandem booster [15]. It has been associated with the stretched $\pi p_{3/2}\nu g_{9/2}^2$ configuration. The data set used in the present analysis was also obtained in a deep-inelastic experiment performed at Argonne National Laboratory. The prompt $\gamma$ rays proposed to feed the 19/2$^-$ isomeric state were identified by setting double coincidence gates on known delayed transitions depopulating the isomer. Because excited levels above isomeric states in nuclei located in the vicinity of magic nuclei occur by breaking either the proton or the neutron core, the observation in the present work of two states beyond the 19/2$^-$ isomer is expected to add important information concerning the size of the $Z = 28$ shell and $N = 40$ subshell gaps.

## II. EXPERIMENT

Excited levels in $^{71}$Cu were populated in the reaction of a 430-MeV $^{64}$Ni beam with a 55 mg/cm$^2$, isotopically enriched $^{238}$U target. The beam was produced by the ATLAS accelerator at Argonne National Laboratory. Gamma rays emitted by the reaction products were detected by the Gammasphere array consisting of 100 Compton-suppressed HPGe detectors [16]. The beam was bunched in pulses separated by 410-ns intervals. Delayed $\gamma$ rays could be studied between these beam pulses. The trigger condition required at least three suppressed Ge detectors to fire in coincidence. The data were sorted in

 ©2009 The American Physical Society

coincidence cubes corresponding to different $\gamma$-ray times with respect to the prompt beam burst. Four such cubes combining prompt (P) and delayed (D) $\gamma$ rays were obtained. Transitions were considered to be prompt if they were registered within $\pm 20$ ns of the beam burst. The delayed events were acquired during the ~400 ns period between pulses and arose partly from the decay of isomeric states. More details about the sorting procedure and data analysis are given in Refs. [17] and [18] where the same experimental techniques were employed to study the level schemes of neutron-rich Fe isotopes. In the present analysis, the DDD cube was used for the investigation of the transitions depopulating the $19/2^-$ isomer, while the double gates set in the PDD and PPD coincidence histograms helped identify the prompt $\gamma$ rays feeding this isomer.

## III. EXPERIMENTAL RESULTS

As mentioned in the Introduction, the $19/2^-$ isomer in $^{71}$Cu was identified in two independent deep-inelastic reactions performed at the JAERI tandem booster and at GANIL. In the JAERI experiment, a $^{198}$Pt metal foil was bombarded with a $^{76}$Ge beam at an energy of 635 MeV [15]. The $19/2^-$ isomer produced in this way was found to decay to the ground state via a cascade of four $E2$ transitions defining the $19/2^- \rightarrow 15/2^- \rightarrow 11/2^- \rightarrow 7/2^- \rightarrow 3/2^-$ sequence. Almost at the same time, the $19/2^-$ isomer in $^{71}$Cu and its $\gamma$ decay were also identified by Grzywacz *et al.* [14] among the reaction products of a 60.3/u-MeV $^{86}$Kr beam on a $^{\mathrm{nat}}$Ni target. In both runs, the experimental setup consisted of five Ge detectors surrounding Si detectors used to detect the implanted fragments [14,15]. The deexcitation of isomers produced in the reactions was studied in each experiment by correlating the implanted ions with the subsequent $\gamma$ decay. A half-life of $T_{1/2} = 0.275(14)$ $\mu$s was measured in Ref. [14], which proved to be in very good agreement with the $T_{1/2} = 0.25(3)$ $\mu$s value determined in Ref. [15] from the analysis of the decay curves of the intense $\gamma$ rays deexciting the isomer.

In the present analysis, the transitions reported previously were used to set double gates in the coincidence cubes. Figure 1 provides the coincidence spectrum obtained by gating on the delayed 133- and 495-keV $\gamma$ rays depopulating the

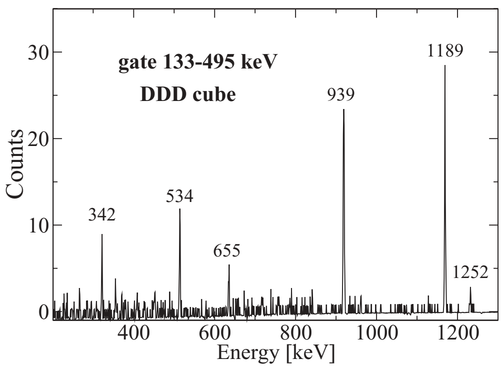


FIG. 1. $\gamma$-ray spectrum from the 133- to 495-keV coincidence gate in the DDD cube. Transitions marked by their energies belong to the level scheme of $^{71}$Cu.

$19/2^-$ isomer. The two transitions have energies similar to the $8^+ \rightarrow 6^+$ and $6^+ \rightarrow 4^+$ cascade in the even-even $^{70}$Ni core and, therefore, were assigned the spin sequence $19/2^- \rightarrow 15/2^- \rightarrow 11/2^-$ [14,15]. According to Refs. [14,15], the $11/2^-$ level deexcites toward the ground state via a main decay path consisting of the 939- and 1189-keV transitions, as well as through a cascade of three $\gamma$ rays with energies 342, 1252, and 534 keV. Our coincidence data are in agreement with the proposed deexcitation paths (see Fig. 1). Grzywacz and collaborators, however, suggested a third decay branch consisting of three $\gamma$ rays of energies 495, 652(2), and 981 keV through excited levels at 1633 and 981 keV [14]. The results of the $\beta$-decay work by Franchoo *et al.* [4,19] confirmed only the presence of the 981-keV level. A spin $7/2^-$ is proposed for this state, based on the observed deexcitation pattern and a comparison with particle-core calculations [20]. The 981-keV state was found to decay to the $3/2^-$ ground-state directly via the 981-keV $\gamma$ ray and through a pair of weak transitions at 447 and 534 keV [4,19].

Here this 447- to 534-keV cascade was used to place double gates in the DDD cube. The resulting spectrum does not contain the 495- and 652(2)-keV transitions proposed by Grzywacz *et al.* [14]. Instead, the spectrum showed clear evidence for the presence of the 472- and 521-keV $\gamma$ rays, also observed in $\beta$ decay and proposed to deexcite the levels at 1453 and 1974 keV [19]. Particle-core calculations suggested spins and parities of $9/2^-$ and $11/2^-$ for these states that, together with the 981-keV level discussed above, were interpreted to belong to the band built on the $\pi f_{7/2}^{-1}$ hole configuration [20].

Prompt transitions feeding the $19/2^-$ isomer were investigated by analyzing the PDD cube. In this histogram, the spectrum of prompt radiation is obtained when setting double gates on any two delayed transitions below the isomer. The analysis of the PDD cube showed clear evidence for the presence of the prompt 2020-keV coincident $\gamma$ ray [see Fig. 2 (left)]. Furthermore, the double-gate set on the prompt 2020-keV and delayed 1189-keV transitions resulted in the spectrum displayed at the right of Fig. 2, where the observation of the coincident 133-, 495- and 939-keV $\gamma$ rays gives confidence that the newly observed 2020-keV transition belongs indeed to the level scheme of $^{71}$Cu. Owing to its intensity and the absence of other $\gamma$ rays, except the weaker 554-keV line discussed below, this transition is proposed to feed directly the $19/2^-$ isomer, and therefore, it is placed in the $^{71}$Cu level scheme as deexciting the 4776-keV state (see Fig. 3).

Levels beyond the newly observed 4776-keV state were investigated further by setting double gates in the PPD cube. The analysis of the coincidence relationships by using any of the delayed transitions depopulating the $19/2^-$ isomer and the prompt 2020-keV line showed evidence for the prompt 554-keV $\gamma$ ray that is placed in the $^{71}$Cu level scheme as depopulating a level at 5330 keV (see Figs. 3 and 4).

No transitions other than those placed in the level scheme of Fig. 3 could be identified in the analysis of the present data set. The investigation of the PPP cube by placing double gates on the delayed transitions placed in the level scheme of Fig. 3 as well as those observed in the $\beta$ decay of the $^{71}$Ni isobar [19] did not reveal any further information. This indicates that the observation of $\gamma$ rays in $^{71}$Cu produced in

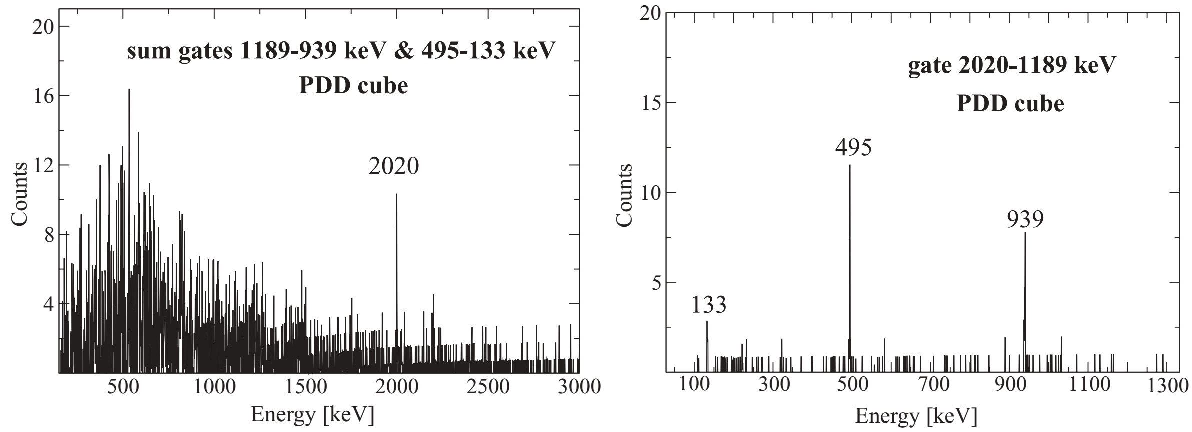


FIG. 2. (Left) Summed $\gamma$-ray spectrum from the 1189- to 939-keV and 495- to 133-keV coincidence gates in the PDD cube showing the 2020-keV $\gamma$ ray assigned in the present work to the level scheme of $^{71}$Cu. (Right) Coincidence spectrum obtained by placing the 2020- to 1189-keV double gate in the PDD cube (see text for a detailed discussion).

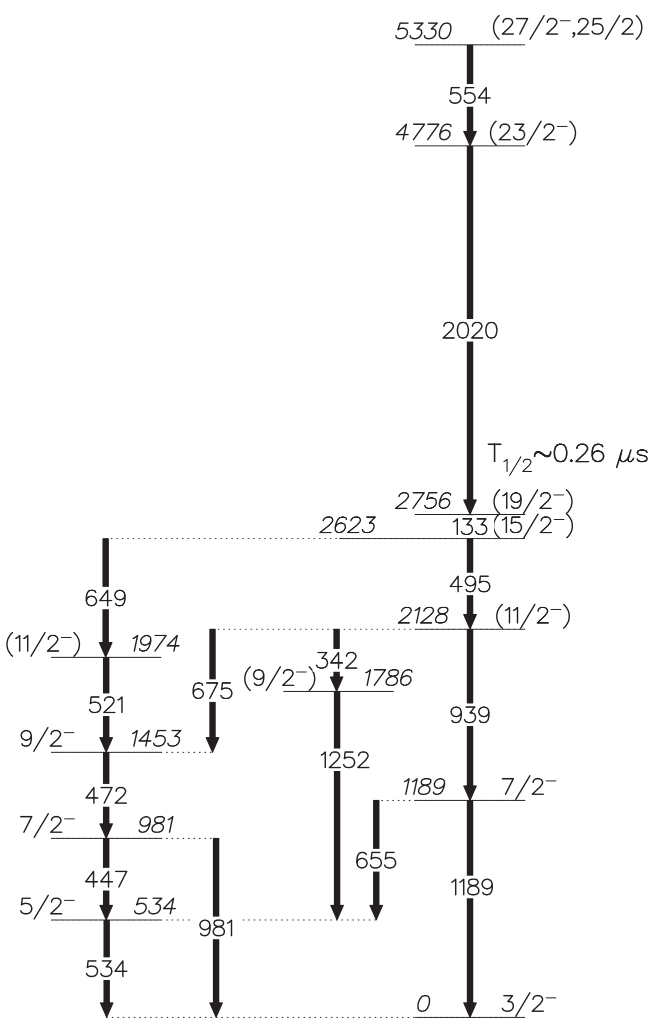


FIG. 3. Level scheme for $^{71}$Cu obtained in the present work. The levels below the 19/2$^{-}$ isomer were reported in previous measurements [4,14,15,19] and confirmed by the analysis of the DDD cube in the present experiment. The two $\gamma$ rays feeding the isomer are newly observed.

deep-inelastic reactions depends strongly on the population of the 19/2$^{-}$ isomer because the prompt feeding of the yrast states below it proved to be much weaker.

As the observed levels associated with the main decay path of the 19/2$^{-}$ isomer in $^{71}$Cu were found to resemble closely the positive-parity states in the even-even $^{70}$Ni core [14], the observation of excited states above this 19/2$^{-}$ long-lived state raised the question whether similar levels can also be identified above the 8$^{+}$ isomer in the core nucleus. The latter is also produced in the present deep-inelastic reaction. To address this issue, a similar analysis was performed in $^{70}$Ni. In this case, the statistics observed in the corresponding $\gamma$-$\gamma$ coincidence spectra proved to be a factor of two lower when compared to $^{71}$Cu. The double gates set on known transitions below the 8$^{+}$ isomer in $^{70}$Ni yielded low statistics spectra from which no firm conclusion could be drawn concerning the existence of similar transitions.

The spectroscopic information extracted in the present analysis for the levels observed in $^{71}$Cu is summarized in Table I.

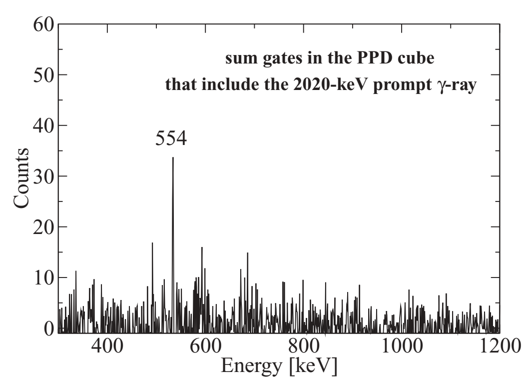


FIG. 4. Summed $\gamma$-ray spectrum from the 1189- to 2020-keV, 939- to 2020-keV, 495- to 2020-keV, and 133- to 2020-keV coincidence gates in the PPD cube illustrating the presence of the 554-keV transition assigned to the level scheme of $^{71}$Cu.

TABLE I. Excitation energies, transition energies, and initial and final spin and parities deduced in $^{71}$Cu. The quoted experimental intensities are extracted from the delayed data and are normalized to the 495-keV transition, set to be 100. The experimental errors on the transitions energies are 0.2 keV for the intense $\gamma$ rays and 0.5 keV for the weak ones ($I_\gamma < 5\%$).

| $E_{level}$ (keV) | $E_\gamma$ (keV) | $I_\gamma$(%) | $I_i^\pi \rightarrow I_f^\pi$ |
|---|---|---|---|
| 534.3 | 534.3 | 21(5) | $5/2^- \rightarrow 3/2^-$ |
| 981.5 | 447.2 | 12(2) | $7/2^- \rightarrow 5/2^-$ |
| | 981.5 | 42(4) | $7/2^- \rightarrow 3/2^-$ |
| 1189.2 | 654.9 | 10(1) | $7/2^- \rightarrow 5/2^-$ |
| | 1189.2 | 96(4) | $7/2^- \rightarrow 3/2^-$ |
| 1453.4 | 471.9 | 51(3) | $9/2^- \rightarrow 7/2^-$ |
| 1786.5 | 1252.2 | 9(1) | $(9/2^-) \rightarrow 5/2^-$ |
| 1974.0 | 520.6 | 48(3) | $(11/2^-) \rightarrow 9/2^-$ |
| 2128.3 | 341.8 | 8(1) | $(11/2^-) \rightarrow (9/2^-)$ |
| | 674.9 | 1.3(4) | $(11/2^-) \rightarrow 9/2^-$ |
| | 939.1 | 69(4) | $(11/2^-) \rightarrow 7/2^-$ |
| 2623.4 | 495.1 | 100 | $(15/2^-) \rightarrow (11/2^-)$ |
| | 649.4 | 52(4) | $(15/2^-) \rightarrow (11/2^-)$ |
| 2756.2 | 132.8 | 15(2) | $(19/2^-) \rightarrow (15/2^-)$ |
| 4776.5 | 2020.3 | | $(23/2^-) \rightarrow (19/2^-)$ |
| 5330.7 | 554.2 | | $(27/2^-, 25/2) \rightarrow (23/2^-)$ |

## IV. INTERPRETATION

The limited statistics obtained for $^{71}$Cu in the present measurement prevent the extraction of reliable angular distribution or correlation data for the 2020- and 554-keV transitions. Therefore, spins and parities cannot be firmly assigned to the newly observed states. Also, as similar transitions have not yet been identified in the neighboring nuclei, spin and parity assignments cannot be proposed based on systematics. However, important information concerning the nature of the levels identified in the present analysis can be derived from the experimental data available for the $Z = 42$, $N = 50$ $^{92}$Mo nucleus [21,22], the counterpart of the $^{70}$Ni core. In other words, considering $Z = 28$ and $N = 50$ as strong shell closures leaves $^{70}$Ni and $^{92}$Mo as two nuclear systems serving as good indicators for the range of spins and excitation energies that can be accommodated by 42 particles of one kind.

In $^{92}$Mo, the observed positive-parity $8^+ \rightarrow 6^+ \rightarrow 4^+ \rightarrow 2^+ \rightarrow 0^+$ cascade exhibits a spacing specific to seniority $\nu = 2$ levels, similar to the yrast cascade in $^{70}$Ni, except that, in $^{92}$Mo, the low-lying states are dominated by proton excitations. Two ~2-MeV $\gamma$ rays were found to feed the $8^+$ isomer in $^{92}$Mo (see Fig. 5 and Ref. [22]). In that work, spin and parity $10^+$ were proposed for the two states, based on the results of a directional correlation analysis and comparisons with shell-model calculations. Theory predicted for both states configurations involving proton excitations from single-particle orbitals below $Z = 40$ to the $\pi g_{9/2}$ orbital, while neutron excitations across $N = 50$ were predicted to be located at higher angular momentum and excitation energy [22].

The excited levels constituting the main decay path of the $19/2^-$ isomer in $^{71}$Cu were found to have energies very

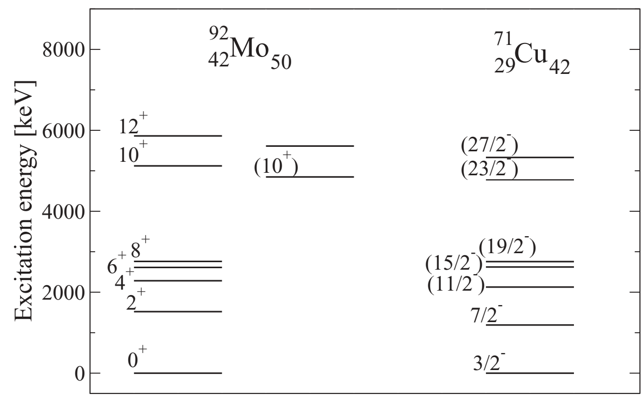


FIG. 5. Comparison between the partial level schemes of $^{92}$Mo [22] and $^{71}$Cu.

similar to the positive-parity yrast states below the $8^+$ isomer in the $^{70}$Ni core, in agreement with the proposed particle-core coupling scheme [14,23]. This indicates that the interaction between the $p_{3/2}$ proton and the valence neutrons is rather weak. It seems, therefore, reasonable to suggest that the levels observed beyond the $19/2^-$ isomer in $^{71}$Cu are dominated by neutron excitations with only a minor contribution from the odd proton. One can extrapolate further and assign spin and parity $23/2^-$ to the newly observed state at 4776 keV, based on the comparison with the observed decay scheme of $^{92}$Mo (see Fig. 5).

Both $10^+$ states observed in $^{92}$Mo were found to be populated by levels located ~0.7 MeV higher in excitation energy. For the strongest of the two transitions associated with the decay of these higher-lying states, the experimental directional correlation ratio indicated an $E2$ character and, therefore, a spin and parity $12^+$ for the emitting level. Coupling the $p_{3/2}$ odd proton to this state would correspond to a spin and parity assignment of $27/2^-$ for the 5330-keV state in $^{71}$Cu (see Fig. 5). However, in the absence of angular correlation information, a $25/2^+$ or $25/2^-$ assignment cannot be ruled out. In particular, a $25/2^+$ level might be expected around this excitation energy and would be associated with a $\pi p_{3/2} \otimes \nu(p_{1/2}^{-1} g_{9/2}^3)_{11^-}$ configuration.

One can further argue that, in the neutron-rich Ni isotopes, states with spins $I > 8$ can also be created by exciting protons across the $Z = 28$ shell gap, which is predicted to decrease as neutrons fill the $g_{9/2}$ orbital [13]. In fact, the large $B(E2; 2^+ \rightarrow 0^+)$ value, measured recently in $^{70}$Ni by Coulomb excitation with radioactive beams, was regarded as evidence for enhanced proton core polarization due to the quenching of the $Z = 28$ shell gap caused by strong $\pi f_{7/2}$-$\nu g_{9/2}$ and $\pi f_{5/2}$-$\nu g_{9/2}$ interactions [9,13]. The predicted quenching, however, was not supported by the recent systematic study of the reduced transition probabilities in the odd-$A$ Cu isotopes with masses $A = 67$–$73$ [23]. In that work, the drop in energy of the low-lying $5/2^-$ and $7/2^-$ states, believed to contain important components from the $\pi f_{5/2}$ and $\pi f_{7/2}$ orbitals, was found to not be accompanied by an increase in the corresponding transition probabilities. In fact, the measured $B(E2; 5/2^- \rightarrow 3/2^-)$ values in the Cu isotopes with $N \geqslant 40$ are consistent

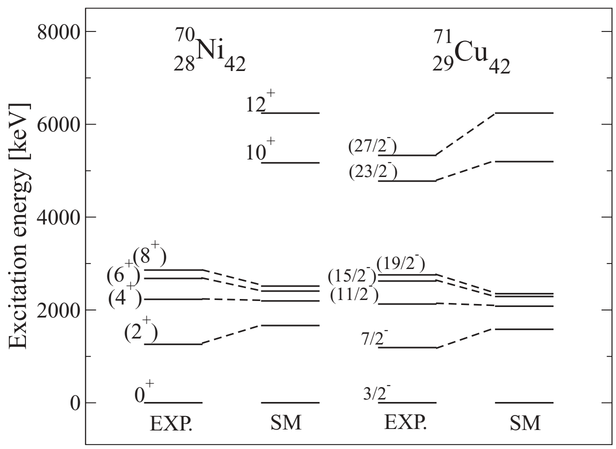


FIG. 6. Partial level schemes of $^{70}$Ni and $^{71}$Cu compared with the results of ANTOINE shell-model calculations (see text for details).

within a factor of two with shell-model predictions, while the population of the single-particle 7/2$^-$ state was not observed, indicating very low collectivity for these levels [23].

In the more likely scenario that the newly observed states arise from breaking the $N = 40$ neutron core, the observed 2020-keV transition feeding the 19/2$^-$ isomer directly can then be regarded as a measure for the energy required to promote an additional pair of neutrons from the $fp$ shell into the $g_{9/2}$ orbital. This energy is very close to the predicted size of the $N = 40$ subshell gap and is also similar to the energy of the $2_1^+$ state in $^{68}$Ni. Thus, the present result can be viewed as a clear indication that the $N = 40$ gap remains a good subshell closure at high excitation energies in $^{71}$Cu. This finding is surprising because the large $B(E2)$ values in $^{70}$Ni and $^{72}$Cu obtained experimentally seemed to indicate that the stabilizing effects of the $Z = 28$ and $N = 40$ gaps are rather localized around $^{68}$Ni and the coupling of at least two like quasi-particles to the $^{68}$Ni core induces large polarization effects [7,9].

The observed positive-parity yrast states in $^{70}$Ni, the main decay path of the 19/2$^-$ isomer in $^{71}$Cu and the newly identified states beyond the isomer are compared with ANTOINE shell-model calculations [24] in Fig. 6. The model uses a realistic effective interaction obtained from the $G$ matrix [25] and modified further for a monopole correction [26]. The same interaction was employed for calculations of the observed low-lying levels and $B(E2)$ values in $^{68-73}$Cu [7,23]. The valence space considered for both protons and neutrons consists of the $fpg$ orbitals outside an inert $^{56}$Ni core, without any restriction on their occupation. This model space should be sufficient to explain states with spins as high as 29/2$^-$ or 31/2$^+$.

The calculation provides a fair description of the energy levels below the 8$^+$ and 19/2$^-$ isomers and predicts a large gap between the 19/2$^-$ and 23/2$^-$ levels, in agreement with the experimental observations. The main component of the wave functions characterizing the levels below the 19/2$^-$ isomer is the $\pi p_{3/2}\nu g_{9/2}^{+2}$ configuration (∼70%). The model indicates that, although the high angular momenta 23/2$^-$ and 27/2$^-$ can be created in several ways within the chosen model space, the main contributions arise from configurations in which the odd proton occupies the $p_{3/2}$ orbital and four neutrons fill the $g_{9/2}$ state. According to the calculations, the associated wave functions combine the $\pi p_{3/2}\nu(p_{1/2}^{-2}g_{9/2}^{+4})$, $\pi p_{3/2}\nu(f_{5/2}^{-1}p_{1/2}^{-1}g_{9/2}^{+4})$, $\pi p_{3/2}\nu(f_{5/2}^{-2}g_{9/2}^{+4})$, and $\pi p_{3/2}\nu(p_{3/2}^{-1}p_{1/2}^{-1}g_{9/2}^{+4})$ configurations with almost equal weights.

## V. CONCLUSIONS

By analyzing a triple-coincidence data set obtained in the deep-inelastic reaction of a $^{64}$Ni beam at 430 MeV with a thick $^{238}$U target, the level scheme of $^{71}$Cu was extended up to an excitation energy of 5330 keV. Two new prompt $\gamma$ rays of energies 2020 and 554 keV are proposed in the present work to feed the 19/2$^-$ isomer arising from the $\pi p_{3/2}\nu g_{9/2}^{+2}$ stretched configuration. A spin of 23/2$^-$ is proposed for the level at 4776 keV with a configuration dominated by neutron excitations from the $p_{3/2}$, $f_{5/2}$, and $p_{1/2}$ orbitals to the $g_{9/2}$ state. While the comparison with the observed level scheme of $^{92}$Mo suggests a spin and parity of 27/2$^-$ for the 5330-keV level, 25/2$^+$ and 25/2$^-$ spin assignments cannot be ruled out. The high energy required to create the additional 2 units of angular momentum beyond 19/2$^-$ indicates that the $N = 40$ subshell gap is still significant in $^{71}$Cu, in contradiction with recent suggestions pointing to a breaking of the $^{68}$Ni core when two or more like quasiparticles are added.

## ACKNOWLEDGMENTS

This work was supported by the US Department of Energy, Office of Nuclear Physics, under Contracts DEFG02-94ER40834 and DE-AC02-O6CH11357 and by Polish Scientific Grant 2PO3B-074-18.

[1] M. Bernas *et al.*, Phys. Lett. **B113**, 279 (1982).
[2] M. Bernas *et al.*, J. Phys. Lett. **45**, 851 (1984).
[3] R. Broda *et al.*, Phys. Rev. Lett. **74**, 868 (1995).
[4] S. Franchoo *et al.*, Phys. Rev. Lett. **81**, 3100 (1998).
[5] W. F. Mueller *et al.*, Phys. Rev. Lett. **83**, 3613 (1999).
[6] O. Sorlin *et al.*, Phys. Rev. Lett. **88**, 092501 (2002).
[7] I. Stefanescu *et al.*, Phys. Rev. Lett. **98**, 122701 (2007).
[8] N. Bree *et al.*, Phys. Rev. C **78**, 047301 (2008).
[9] O. Perru *et al.*, Phys. Rev. Lett. **96**, 232501 (2006).
[10] H. Mach, in *Proceedings of the International Symposium on Nuclear Structure Physics, Göttingen, Germany, 2001* (World Scientific, Singapore, 2001), p. 379.
[11] M. Hannawald *et al.*, Phys. Rev. Lett. **82**, 1391 (1999).
[12] D. Pauwels *et al.*, Phys. Rev. C **78**, 041307(R) (2008).
[13] T. Otsuka, T. Suzuki, R. Fujimoto, H. Grawe, and Y. Akaishi, Phys. Rev. Lett. **95**, 232502 (2005).
[14] R. Grzywacz *et al.*, Phys. Rev. Lett. **81**, 766 (1998).
[15] T. Ishii *et al.*, Phys. Rev. Lett. **81**, 4100 (1998).

[16] I. Y. Lee, Nucl. Phys. **A520**, 641c (1990).
[17] N. Hoteling *et al.*, Phys. Rev. C **74**, 064313 (2006).
[18] N. Hoteling *et al.*, Phys. Rev. C **77**, 044314 (2008).
[19] S. Franchoo *et al.*, Phys. Rev. C **64**, 054308 (2001).
[20] A. M. Oros-Peusquens and P. F. Mantica, Nucl. Phys. **A669**, 81 (2000).
[21] T. Numao, H. Nakayama, T. A. Shibata, and Y. Kuno, Nucl. Phys. **A305**, 163 (1978).
[22] N. S. Pattabiraman *et al.*, Phys. Rev. C **65**, 044324 (2002).
[23] I. Stefanescu *et al.*, Phys. Rev. Lett. **100**, 112502 (2008).
[24] E. Caurier, computer code ANTOINE, IRES, Strasbourg, 1989–2002.
[25] M. Hjorth-Jensen *et al.*, Phys. Rep. **261**, 125 (1995).
[26] F. Nowacki, Ph.D. thesis, IRES, Strasbourg, 1996; F. Nowacki (private communication).